JOURNAL OF SOLID STATE CHEMISTRY 5, 419–431 (1972)

Electron Microscopy of the Niobium Oxides. I. Twinning and Defects in H-Nb_2O_5

J. S. ANDERSON, J. M. BROWNE, AND J. L. HUTCHISON

Inorganic Chemistry Laboratory, Oxford, England

Received November 29, 1971

Two dimensional direct lattice imaging has been used to identify the detailed structure of faults in stoichiometric H-Nb_2O_5 crystals grown under different conditions. Material grown at 1000°C showed occasional twinning on (10$\bar{1}$); only one of two possible twin structures was identified. Material grown at lower temperatures frequently incorporated "wrong sized" blocks, equivalent to inserted lamellae of M- or N-Nb_2O_5. Heavily faulted twinned and intergrown structures are occasionally formed, and in such a regularly and recurrently twinned variant of the H-Nb_2O_5 structure was identified as a microdomain.

In this and some subsequent papers we shall discuss the structure, and particularly the defect structure, of the niobium oxides, as revealed by high resolution electron microscopy. Allpress, in a series of elegant papers (*1–4*) has shown that direct lattice imaging methods furnish a new insight into the ultramicrostructure of some of the related ternary oxides. He has used the lattice images to interpret coherent intergrowths between block structures and to build up the structure of faulted regions of crystal. It is to be expected that the binary niobium oxides, between $NbO_{2.417}$ and $NbO_{2.500}$, would show the same kind of extended defects as the ternary oxides, but charge localization on cations of fixed valency can introduce differences between ternary and binary oxide systems. Electron microscopy of the Nb–O systems provides an opportunity both to clarify the chemistry of the system and to examine the ground rules of faulting in block structures: the types of internal boundary or modified local order that are compatible with perfect stoichiometry and those that involve nonstoichiometry of the crystals.

Phase relations in the Nb–O system are still obscure. Schäfer, Gruehn and Schulte (*5*) listed 14 crystalline modifications of Nb_2O_5 and we have identified at least one additional ordered structure. Reisman and Holzberg (*6*), however, restricting the definition of a "modification" to phases that undergo reversible transitions (melting or enantiotropic transformations) at 1 atm pressure, conclude that only three genuine modifications have been established. They leave open the status of the other forms: whether they are really ternary phases, with a low, stabilizing concentration of a third element, arising from their mode of preparation, or whether they are metastable structures, nucleated and catalytically grown in the presence of impurities. Crystal structure determinations have identified at least three forms, H-, M- and N-Nb_2O_5, as "block structures" in the nomenclature of Roth, Wadsley and Andersson (*7*). That is, they are built up from columns or blocks of ReO_3-like structure, infinite alone one direction (the short *b* axis) and measuring $(m \times n)$ [NbO_6] octahedra in cross section. Across each side face they are joined by shared octahedron edges, to adjacent blocks $(m' \times n')$ octahedra in cross section; the interface has essentially the structure of a crystallographic shear plane defined by the displacement operator $(a/2)\langle 0\bar{1}1\rangle/\{100\}$ relative to the ReO_3 substructure. Block structures thus represent a stage in the hierarchy of organized structures rather more complex than that of the generality of ionic crystals: subject to certain constraints, every combination of block sizes—(m, n), (m', n'), (m'', n''), etc. represents a possible local arrangement of blocks within a crystal. The constraints are (a) that the system of face sharing blocks must be space filling (but may enclose

tunnels that provide tetrahedral sites); (b) that the permitted stable sizes of blocks ($m \times n$) are restricted by the formal charges borne by their constituent ions (Nb^{5+}, Nb^{4+}, ternary elements of lower or higher charge; O^{2-}, OH^- or F^- as anions). This restriction arises from the avoidance of excessive net anionic or cationic charge in any element of the structure. Every combination of block sizes that constitutes a regular repeating pattern generates a discrete crystal structure, i.e., is a distinct compound or crystal modification. Modification of a regular pattern by incorporating "wrong" blocks locally, in coherent intergrowth with the matrix, creates an extended defect or faulted microdomain.

Allpress has shown that these systems are very suitable for study by electron microscopy, and has identified numerous instances of extended defects and fluctuations of composition (out of equilibrium states) in the ternary oxides, involving microdomains or lamellae of wrong blocks. Our aim has been to clarify the chemistry of the binary Nb–O system and to identify the most frequently encountered—i.e., the energetically favored—extended defects in real crystals: modes of twinning, planar defects, permitted wrong block combinations. This paper deals with twinning and defects in stoichiometric H-Nb_2O_5. Gatehouse and Wadsley (*8*) determined the structure of the monoclinic crystals (a, 21.16; b, 3.822; c ,19.35 Å; β, 119°50′) as consisting of blocks (3×4) octahedra in size at $y = 0$, with (3×5) blocks at $y = \frac{1}{2}$ (Fig. 1a); the (3×5) blocks share octahedron edges with each other, to form continuous ribbons. Unshared block corners define tunnels of tetrahedral sites. We symbolize the structure as $(3 \times 4)_1 + (3 \times 5)_\infty$ to denote the connectivity of the blocks and find it convenient to emphasize the ribbon linkages in the schematic representation (Fig. 1b) since this makes faulted relationships clearer.

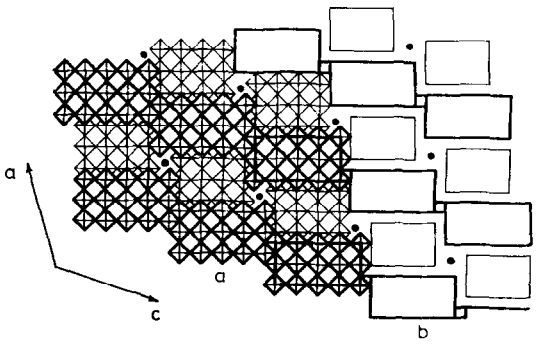

FIG. 1a. Idealized structure of H-Nb_2O_5. Octahedra are outlined and Nb atoms in tetrahedral environment are shown as black dots. (b) H-Nb_2O_5 where blocks are shown as rectangles with edge-sharing also shown.

Experimental Methods

Micrographs are from crystals of H-Nb_2O_5 prepared by chemical vapor transport, using $NbCl_5$ as transport agent, as described by Schäfer, Gruehn and Schulte (*5*). The feedstock was Specpure Nb_2O_5 (Johnson Matthey). Crystals grown at 900–1000°C were, in general, very perfect. Crystals of H-Nb_2O_5 were also one of the main products of transport at 750° → 650°; M- and N-Nb_2O_5 (*9*, *10*), identified by their electron diffraction patterns and lattice images, were also formed in the reaction. It is not clear whether specific impurities, introduced during the chemical vapor transport, could have steered the crystallization process towards the production of these forms (as suggested by Reisman and Holtzberg), and it would appear that metastable modifications can be nucleated and grown during chemical vapor transport. The status of H-Nb_2O_5 formed at 650°C is therefore uncertain; the crystals formed were, in some cases, highly disordered (see below).

For microscopy, crystals were crushed between glass slides, and the powder was transferred to carbon coated copper grids. A JEM 100-U microscope was used, with 100 keV electrons, at a primary magnification of 200,000×, using a high resolution (10° tilt) gonimeter stage. A 60 μm objective aperture was used for lattice imaging. Only a small proportion of the crystals could be brought into the requisite [010] orientation; of these, only a smaller number were thin enough for good 2-dimensional lattice imaging. It must be emphasized that lattice imaging methods involve the problem of what constitutes a representative sample of the material examined. Since exposure times of up to 10 sec may be required, image

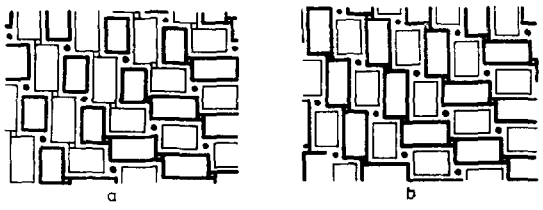

FIG. 2. Possible (10$\bar{1}$) twin boundaries in H-Nb_2O_5, based on idealized models.

stability imposes a further limiting factor on successful lattice image microscopy.

Faulted regions were analyzed by measurement of fringe displacements and contrast features right up to the fault. Although the coordination octahedra are irregular and the niobium atoms displaced from their centers by polarization, little error is introduced by idealizing the structures. Dimensions and directions are then uniquely determined by the octahedron diagonal dimension, ~4A; structural changes displace octahedron centers by multiples of the half-diagonal, 2A, which is about the precision of the measurements.

Results

($10\bar{1}$) *Twinning.* In all block structures, the ReO_3 substructure is conserved with minimum distortion. It follows that twinning is possible only if the structure can be reflected across some composition plane that coincides with (100), (001) or {101} of the ReO_3 structure; the structure

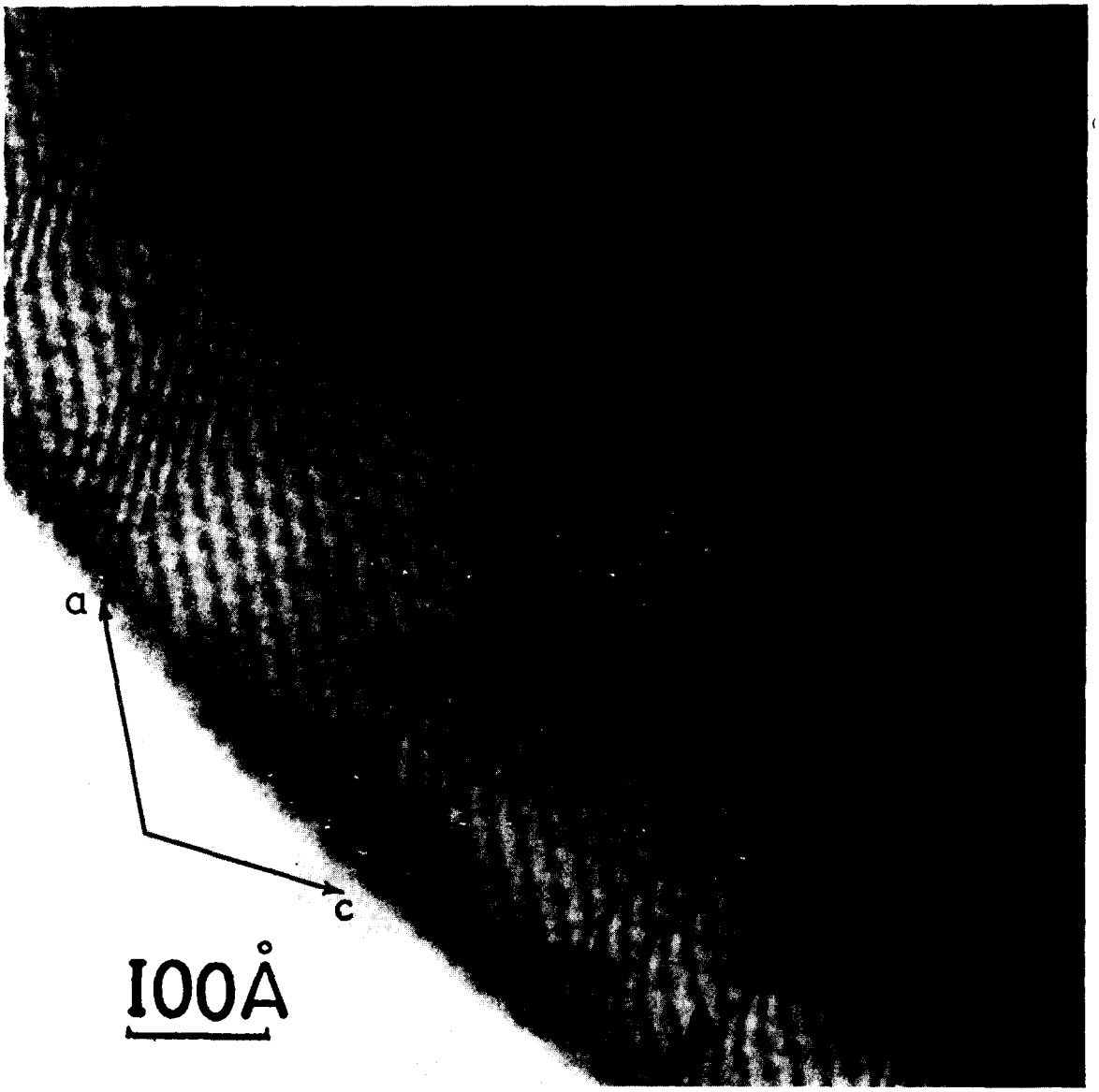

FIG. 3. ($h0l$) lattice image of H-Nb_2O_5, showing ($10\bar{1}$) twin lamellae. Those marked (A) are only 1 unit cell wide.

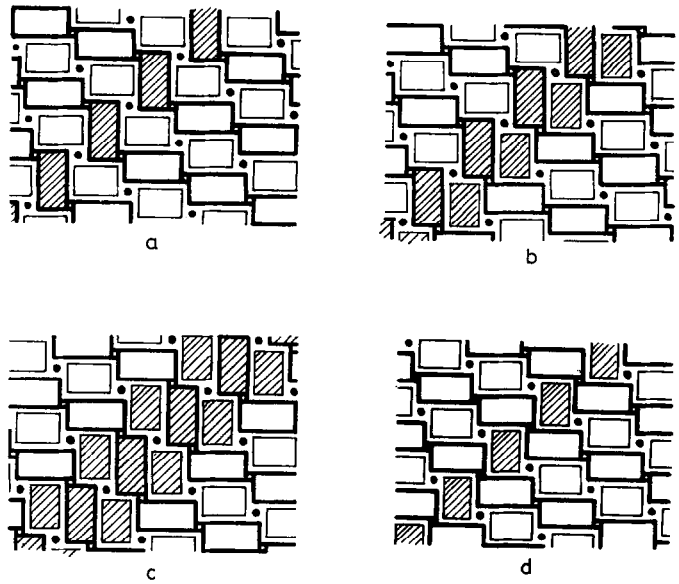

FIG. 4. Possible structures of "single twin lamellae."

in the twin boundary necessarily involves an abnormal juxtaposition of blocks. The constraint implies that not all block structures can undergo twinning, at least without interpolating extended defects. In the case of H-Nb_2O_5, the $(10\bar{1})$ plane provides the only permitted twin boundary (on $(10\bar{1})$ of the ReO_3 substructure); extensive geometrical investigation has shown that there are just two structures (Fig. 2a and b) that could be adopted in simple twinning. Observations on numerous crystals of H-Nb_2O_5 show that simple twinning is not infrequent, and the twins appear to be always of the same type. Figure 3 shows a crystal with twin lamellae of $(10\bar{1})$ orientation, varying in width from over 60A to just under 20A between boundaries. The latter (A, Fig. 3) are of diagnostic interest: they are only 1 unit cell wide and it can be shown that only the mode of Fig. 2b, with the $(3 \times 5)_\infty$ ribbons continuous but folded twice at successive linkages, could accommodate such a narrow reversal of the structure. We find that faults involving folding occur frequently in ribbon structures and it is of some interest to identify the ways in which blocks may be linked at the same level. In H-Nb_2O_5, the $(3 \times 5)_\infty$ ribbons could be recurrently folded in four ways; these differ in the way the adjacent $(3 \times 4)_1$ blocks are fitted in, and they generate different displacements in (100) and (001) fringes as they cross the twinned strip (Fig. 4). In 4d, the (5×3) ribbon is kinked and the array of (4×3) blocks folded; this is better described in terms of crystallographic shear on $(10\bar{1})$ than as a recurrently twinned structure. For the twin lamellae A (Fig. 3) the fringe displacements are consistent with the structure 4a, with only (3×5) blocks reversed. In Fig. 5 (another crystal of H-Nb_2O_5), defect A is of the same type but across B the displacements suggest reversal of one row of (3×4) blocks only.

Intergrowth Faults. M-Nb_2O_5 has a structure based on (4×4) blocks, which can (in principle) be coherently fitted to the H-Nb_2O_5 structure. Since the H-Nb_2O_5 structure could be propagated from a lamella of (4×4) blocks in two orientations, a $(10\bar{1})$ oriented lamella of M-Nb_2O_5 units could give rise to a twinned relationship between the adjacent slabs of H-Nb_2O_5. Three potential structures can be drawn for such a boundary, but we have not observed twins generated in this way.

We have, however, found single sheets of (4×4) blocks, on $(10\bar{1})$ without twinning, in H-Nb_2O_5 crystals grown by chemical vapor transport at low temperatures (e.g., 650°C): they have not been observed in crystals grown or annealed at 1000°C. Figure 6 shows a $(h0l)$ section with two rows of (4×4) blocks, (A, B) clearly identified and confirmed by measurements. In principle, these boundaries might have one of three hypothetical structures: (a) (4×4) blocks linked on both sides to (5×3) blocks—virtually an insertion of M-Nb_2O_5 0.5 unit cell wide

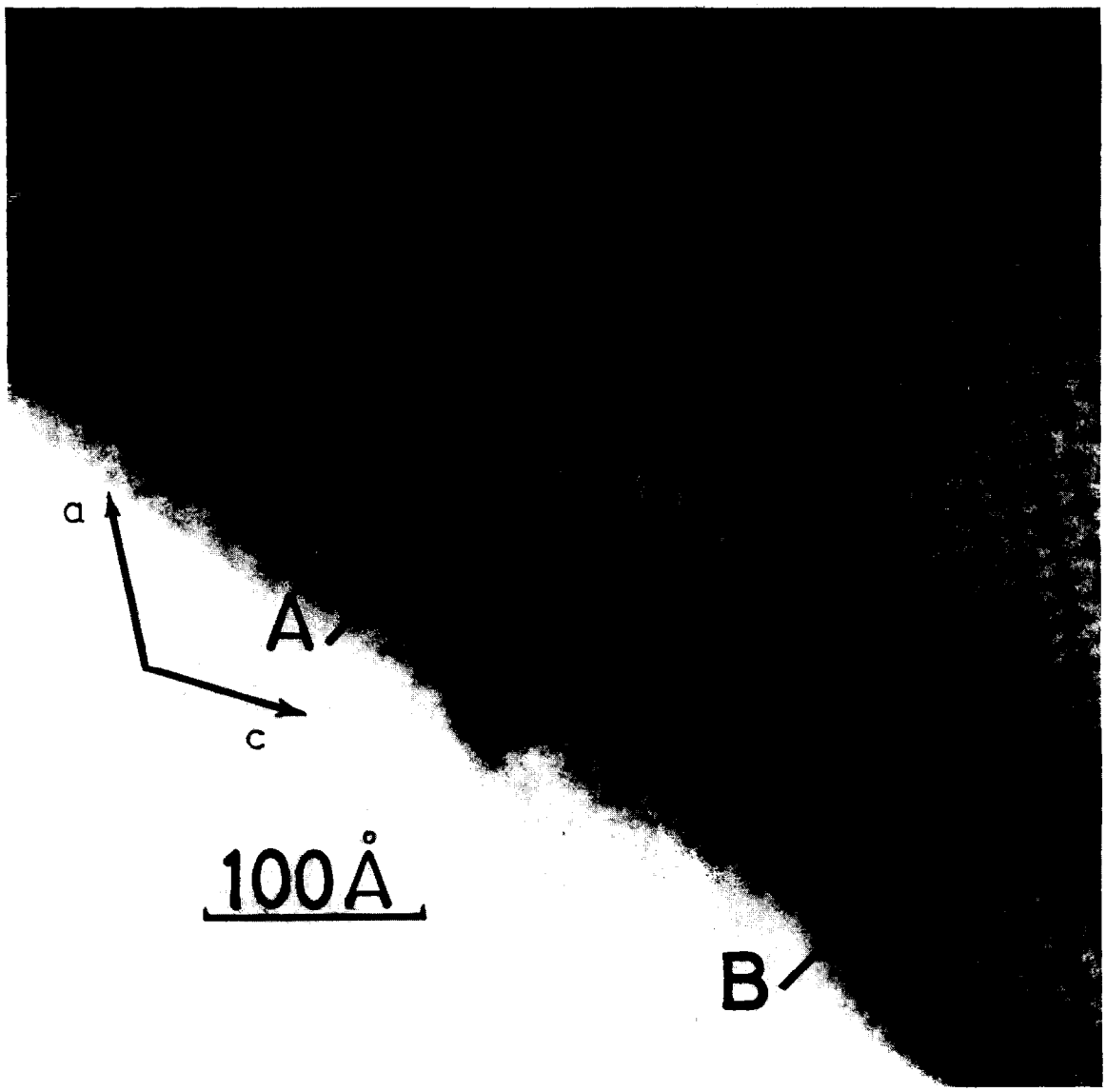

FIG. 5. (*h0l*) lattice image of $H-Nb_2O_5$ showing effect of buckling on the fringe contrast. Single unit cell twins ($10\bar{1}$) are shown at (A) and (B).

(Fig. 7a); (b) (4×4) blocks replacing $(4 \times 3)_1$ blocks—0.5 unit cell strip of $M-Nb_2O_5$ (Fig. 7b); (c) (4×4) blocks linked on one side to (5×3) blocks, and at the same level as the $(4 \times 3)_1$ blocks across the boundary (Fig. 7c). In this case the two block systems are displaced by $\frac{1}{2}b$ across the fault. These possibilities can be distinguished by the breadth of the associated ($10\bar{1}$) fringe spacing and the displacement of the (001) fringes across the fault: for (a) 34A and 5A, respectively, for (b) 20A and about 1A, for (c) 27A and 3.5A.

Measurements of Fig. 6 suggest that both A and B are of the kind shown in Fig. 7c. Analysis of the faults labeled X and Y, at which the lines of (4×4) blocks are displaced sideways (in opposite senses) confirms this. At X the displacement is 9A along [$10\bar{1}$]; the arrangement of Fig. 8a is everywhere consistent in dimensions with measurements made around the fault. The area within the small rectangle—the actual side step—can be regarded as a 0.5 unit cell of $N-Nb_2O_5$. The side step fault Y probably has the structure of

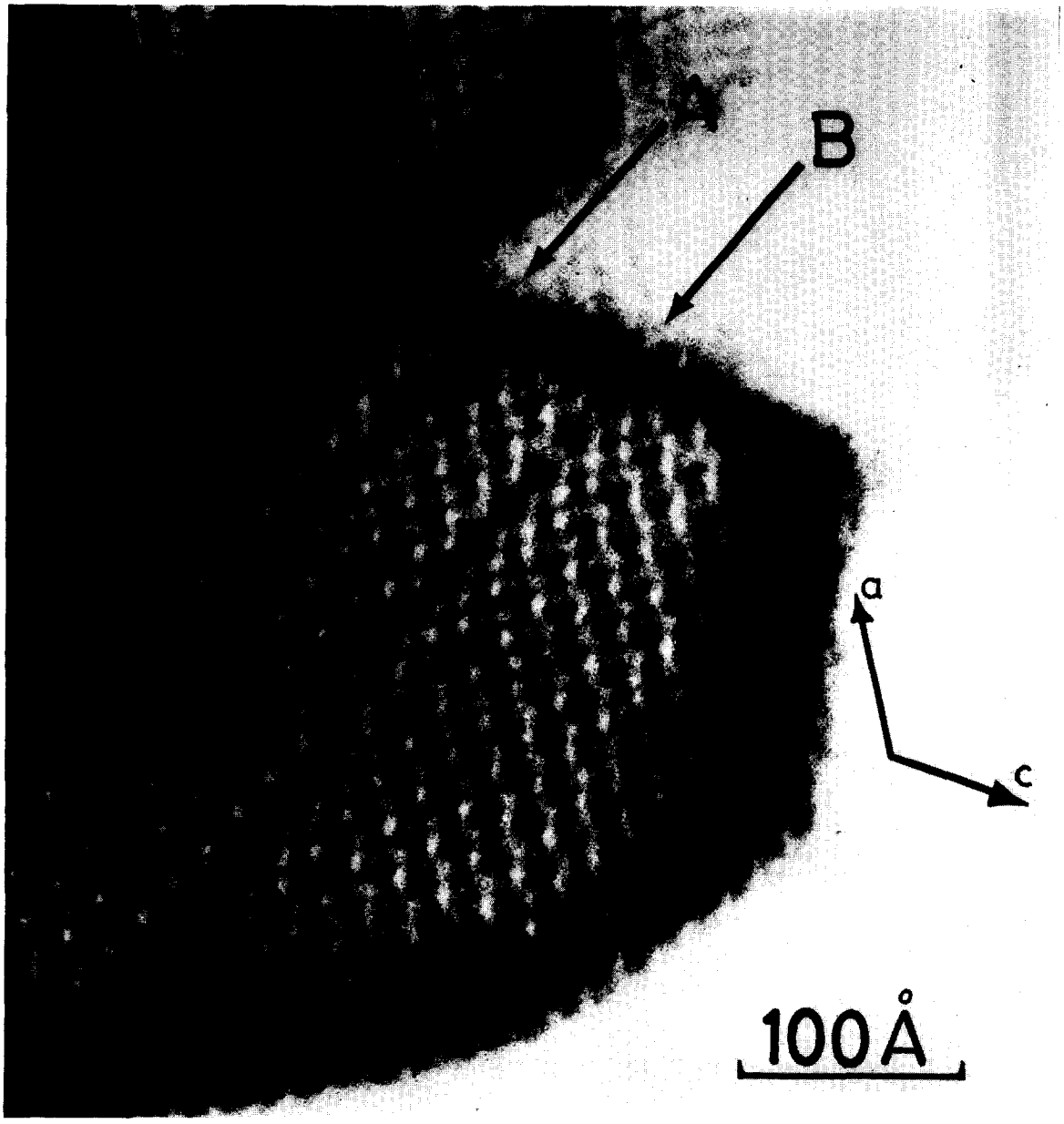

FIG. 6. ($h0l$) lattice image of H-Nb_2O_5 with intergrowths of M-Nb_2O_5 at (A) and (B).

Fig. 8b, again compatible with the detailed measurements. In this fault, one $(4 \times 3)_1$ block inescapably has to be replaced by a $(3 \times 3)_1$ block. This implies a local deviation from stoichiometry: reduction, or segregation of foreign ions. At both X and Y, the (4×4) blocks are displaced by $\frac{1}{2}b$ at the side step.

Defects parallel to a. Faulting is not confined to the $(10\bar{1})$ twin plane but is occasionally found on other orientations. Figure 9 shows a fragment of H-Nb_2O_5 with a single band of diminished contrast X, parallel to a. That this is a block linkage fault, and neither a fortuitous contrast effect nor entirely attributable to a jog along the b direction, is shown by a 5A displacement of the $(20\bar{1})$ fringes across it. We suggest that this band, 32A wide, can be interpreted as a strip along which the $(5 \times 3)_\infty$ ribbons are kinked (Fig. 10). This

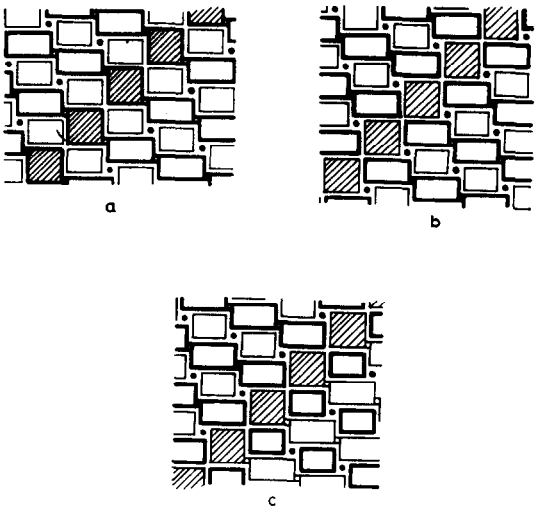

FIG. 7. Possible unit cell wide intergrowths of M-Nb_2O_5 with H-Nb_2O_5.

eliminates tetrahedral sites, thereby modifying the fringe contrast; it also changes the local stoichiometry (to $M_{55}X_{136}$). This would imply either the localized incorporation of univalent anions (OH^- or halogen from the transport reaction) in place of O^{2-} or, less probably, accumulation of anion vacancies.

Domain Intergrowth. Crystal growth by chemical vapor transport at low temperatures occasionally produces highly disordered material. One such crystal, grown at 650°C, is shown at Fig. 11; a good through focus series was available and much of the structural detail could be interpreted on the lines indicated above. The *a* and *c* directions of the H-Nb_2O_5 matrix (and hence the orientation of the ReO_3-type substructure) were fixed by the selected area diffraction pattern, which showed pronounced streaking indicative of disorder along [10$\bar{1}$]. Magnification could be accurately calibrated by measuring the lattice fringes in areas of perfect H-Nb_2O_5 structure. Dimensions of contrast features—e.g., in the regions labeled A, B, C—could then be accurately obtained.

Faulted regions and domains of other structures could then be identified as follows:

i. (10$\bar{1}$) twins: labeled T.

ii. Areas A. Contrast in these is regularly periodic in two directions, 14A × 14.5A including an angle of 105°: the 14A repeat direction is parallel to the ReO_3 substructure axes. The "unit cell" so defined is compatible (as a block

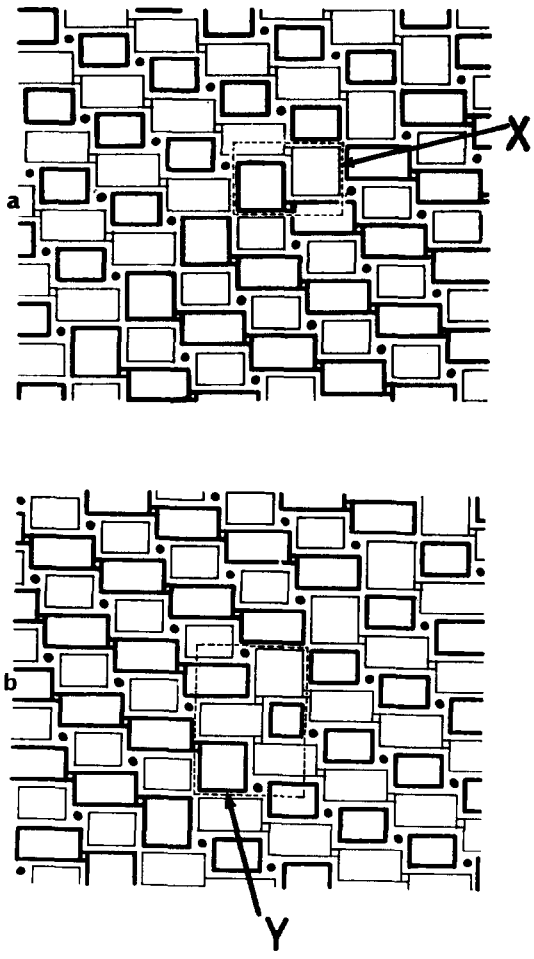

FIG. 8a. Structure of intergrowth (A) in Fig. 6. The region (X) may be regarded as a microdomain of N-Nb_2O_5. (b) Structure of intergrowth (B) in Fig. 6. Note the (3 × 3) block in region (Y) which alters the local stoichiometry.

structure) only with (4 × 4) blocks linked as in N-Nb_2O_5 (Fig. 12); the crystallographic unit cell (shown) has dimensions *a*, 28.51; *b*, 3.830; *c*, 17.48A; β, 124.8° (*10*).

iii. Areas B. Analogy between the structures of N-Nb_2O_5 and $Nb_{12}O_{29}$ (11) suggests that N-Nb_2O_5 should twin on (001). Analysis of the areas B shows that they consist of N-Nb_2O_5 in the mirror image orientation to areas A (Fig. 12); the two orientations are intergrown in several regions. Although the lattice images of areas B show the correct geometry, their contrast is quite different from that of N-Nb_2O_5 in areas A. Such effects could arise from a slight deviation of the electron beam from the exact [010] direction, in that one twin would then be oriented slightly

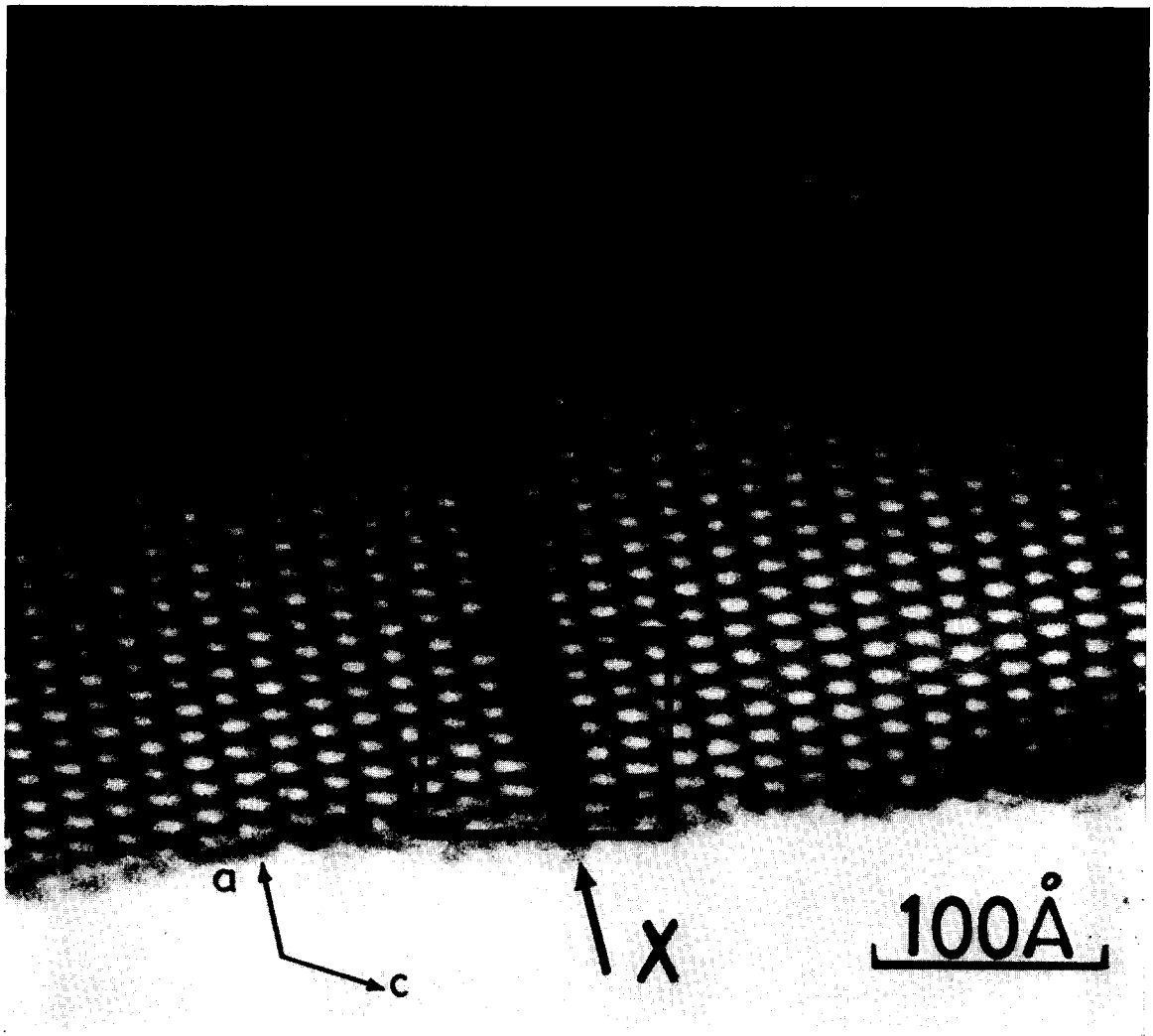

FIG. 9. (*h0l*) lattice image of H-Nb_2O_5, showing a planar defect (X) parallel to *a*.

differently from the other with respect to the beam direction. Coherent intergrowth between N-Nb_2O_5 and H-Nb_2O_5 (not illustrated) is severely restricted by an inherent mismatch in block sizes. We have not found it possible to formulate any interface giving coherence over lengths of more than about 50A. The line XY is probably such an interface, on (20$\bar{1}$) of H-Nb_2O_5 [see (v)].

iv. Area C. This has a well-defined periodicity; its repeating unit of pattern is an oblique cell measuring 19.8A in a direction parallel to (10$\bar{1}$) of H-Nb_2O_5 and 17.5A in a direction inclined at 99° thereto. These measurements, confirmed from the through focus series, do not accord with any block structure yet recognized. On the premiss that corresponding contrast features locate equivalent elements of the structure, and the trial hypothesis that there are tetrahedral sites, a dimensionally consistent structure can at once be deduced. This is related to that of H-Nb_2O_5, but with the $(5 \times 3)_\infty$ ribbons recurrently folded at every block junction and the $(4 \times 3)_1$ blocks in constant orientation (Fig. 13). Within the small domain C its structure is quite regular and (assuming that the *b* axis is one octahedron deep) it could be assigned a monoclinic cell with *a*, 34.7; *b*, 3.8; *c*, 19.8 A; β, 99.4. Although not hitherto observed in bulk or in domains large enough to yield distinguishable electron diffraction patterns, this is potentially a new modification of Nb_2O_5, related to H-Nb_2O_5

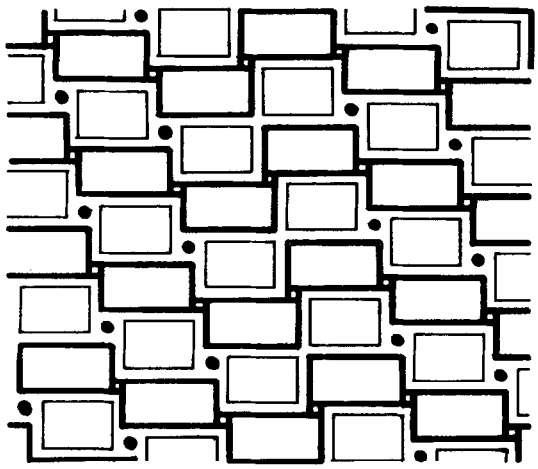

FIG. 10. Structure of the defect (X) in Fig. 9. The diagram shows the detailed structure enclosed by the rectangle in Fig. 9.

in the same way that orthorhombic $Nb_{12}O_{29}$ is to the monoclinic form.

Intergrowth with H-Nb_2O_5 is perfectly coherent, since this regular structure is derived by recurrent twinning on $(10\bar{1})$ (type Fig. 5a). A coherent interface can also be formulated, over a restricted length, because of mismatch in block sizes, between the $(20\bar{1})$ of this structure and (001) of N-Nb_2O_5. Such an intergrowth, over a limited length, is shown in Fig. 11 along the right hand boundary of C.

v. Structureless areas, labeled D. No resolved structure whatever can be seen in several areas of the crystal. These are all adjacent to extended intergrowths of N-Nb_2O_5 and can probably be associated with the inevitable incoherency referred to above. It is clear that organized block structure is lost in these regions. They may represent either genuinely disordered regions or domains of one of those other modifications (e.g., B-Nb_2O_5) which lack characteristic long spacings and, additionally, may be intergrown with the ReO_3-type matrix in some unsuitable orientation, so that they are unresolved. Figure 11 affords further evidence of distortion associated with these structureless areas and mismatch boundaries: close examination reveals that perfect orientation is lost in the adjacent block structure. The rows of octahedra must be locally warped.

The structural features described in this paper are undoubtedly out-of-equilibrium, "non-thermodynamic" defects. They represent, however, the types of extended defect to be found in "as grown" crystals, and they constitute boundaries or discontinuities which may be significant for transport and other properties that are normally treated in terms of an idealized, truly periodic structure. Analysis of such faults has shown that not all the geometrically possible modes of faulting are realized. Evidence is thereby provided that there is some discrimination between modes of faulting, arising either from rather fine energetic differences or through the processes involved in crystal growth.

Appendix: The Interpretation of Lattice Images

Direct lattice imaging methods involve the Fourier transform of a rather small number of reciprocal lattice points, since the number of beams that can be used is restricted by the aberrations of the objective lens. Two dimensional images are formed by combining a finite number of fringe systems: their detail and resolution depend on several factors. (i) Contrast depends upon the focusing of the objective lens (*12–14*). All the micrographs are taken from through-focus series. (ii) Extinction distances differ for reflected beams traversing the crystal in different directions, hence variations in specimen thickness lead to changes in the fringe contours and resulting image contrast distribution (*15*). (iii) The relative intensity of different diffracted (*hkl*) beams depends critically on the orientation of the crystal. Small deviations from the exact [010] orientation weight certain Fourier components and result in asymmetric fringes. Such effects can be observed in some of the accompanying micrographs, in the contrast changes arising from bending of the crystal or from tilting it slightly away from [010]. Figure 14, a through-focus series of a wedge shaped crystal of H-Nb_2O_5 with the electron beam along [010], shows the effects of variations in both thickness and focal conditions. Strong (100), (001) and $(10\bar{1})$ fringe systems are clearly defined and a wealth of finer detail is also resolved. At this scale of resolution, it is not possible to make a one-to-one correlation of image detail with the projected structure of H-Mb_2O_5: calculated 2-dimensional fringe profiles are needed. Such calculations, based on the phase-grating approximation of Cowley and Moodie (*16*), have been carried out for H-Nb_2O_5 by Chidzey (*17*), and the agreement between her computed contrast distribution and the micrographs is encouraging.

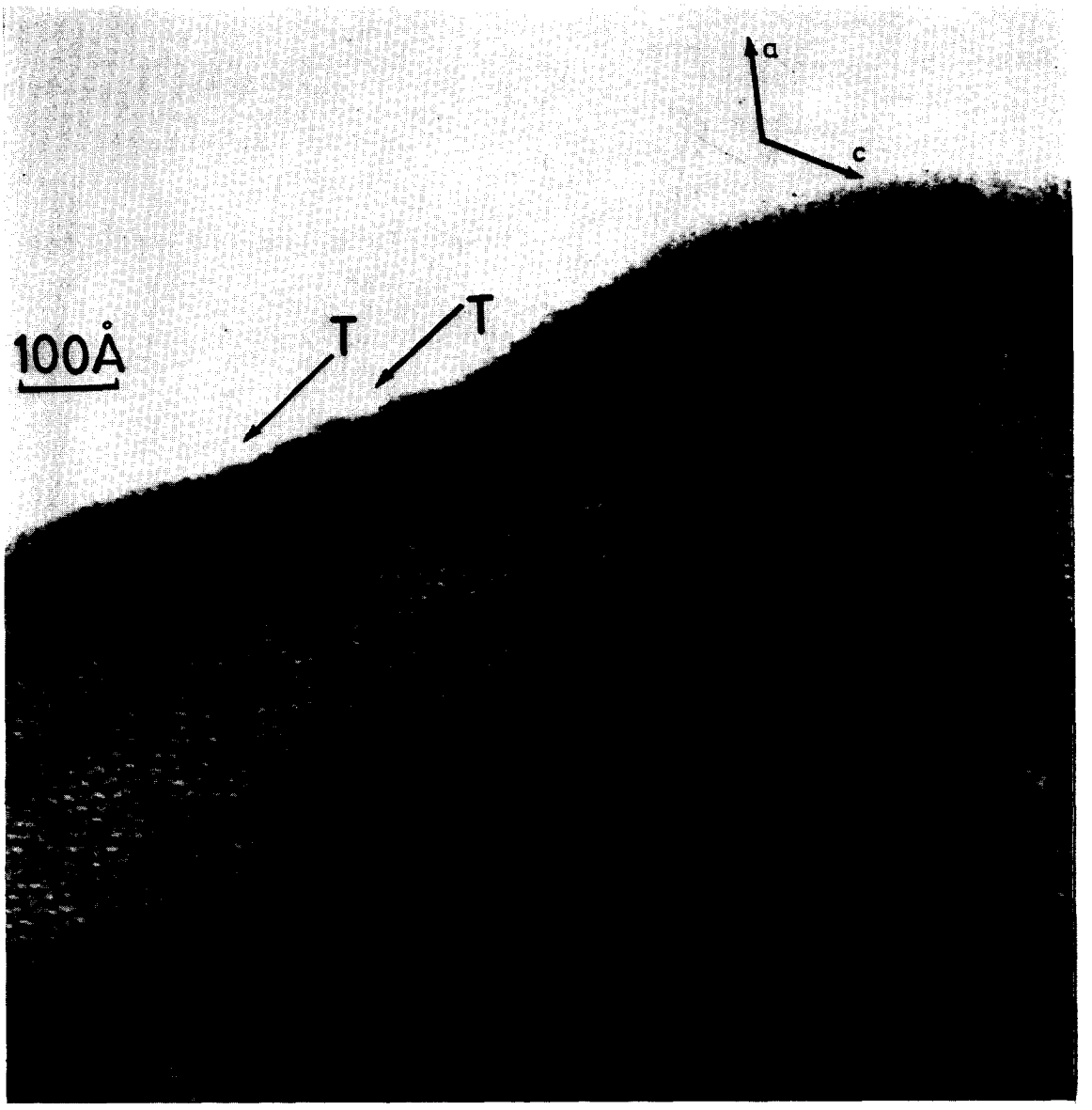

FIG. 11. (*h0l*) lattice image of highly disordered "H-Nb_2O_5," with numerous intergrowths.

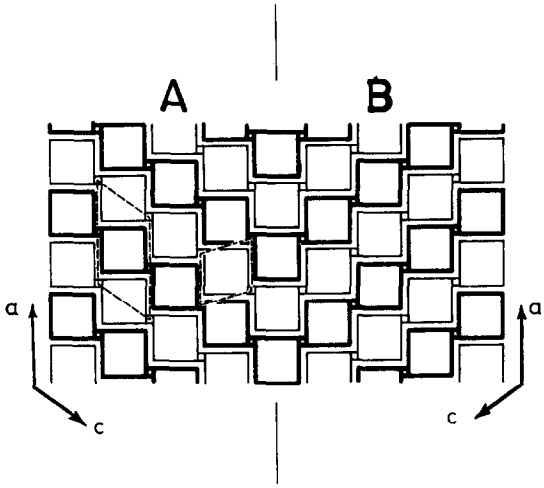

FIG. 12. Structures of N-Nb_2O_5 and N′-Nb_2O_5, the mirror-image form, as observed in areas (A) and (B), respectively, in Fig. 11. The true unit cell and the lattice image repeat unit are shown as X and Y, respectively.

At a more qualitative level, firm inferences can be drawn. The periodic lattice images must agree in dimensions and symmetry with the planar cell that is defined by the periodicity of the crystal. Identical contrast features in the unit cells of the micrograph thus correspond to identical structural features in different unit cells of the crystal, even though the relation between a specific contrast feature of the image and a specific structural feature of the crystal projection remains unspecified. This assumption is more general than that of Allpress (*18*) in his study of 2-dimensional lattice images of $TiNb_{24}O_{62}$ and other compounds where, as a working hypothesis, dark dots on the image were adopted as representing the location of tetrahedral sites. For certain crystal thicknesses and focal conditions, the Allpress assumption appears to be reasonable; under other conditions, fringe contrast may be reversed, and a consistent interpretation of the image is then possible only if white dots are identified with tetrahedral sites (*4*). Recent work by Cowley and Iijima (personal communication) suggests that, for ($h0l$) images of very thin crystals, taken at an appropriate value of defocus, and with the highest attainable resolution, there

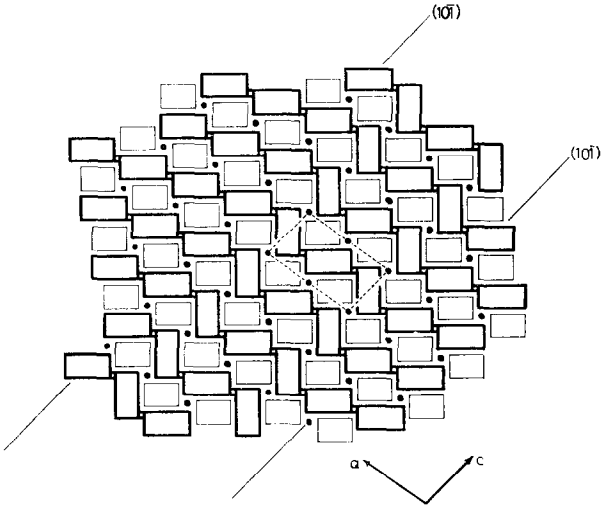

FIG. 13. Structure of a new form of Nb_2O_5 in which the $(3 \times 5)_\infty$ ribbons are regularly and recurrently folded at each block junction. Coherent intergrowth with H-Nb_2O_5 on (10$\bar{1}$) is illustrated.

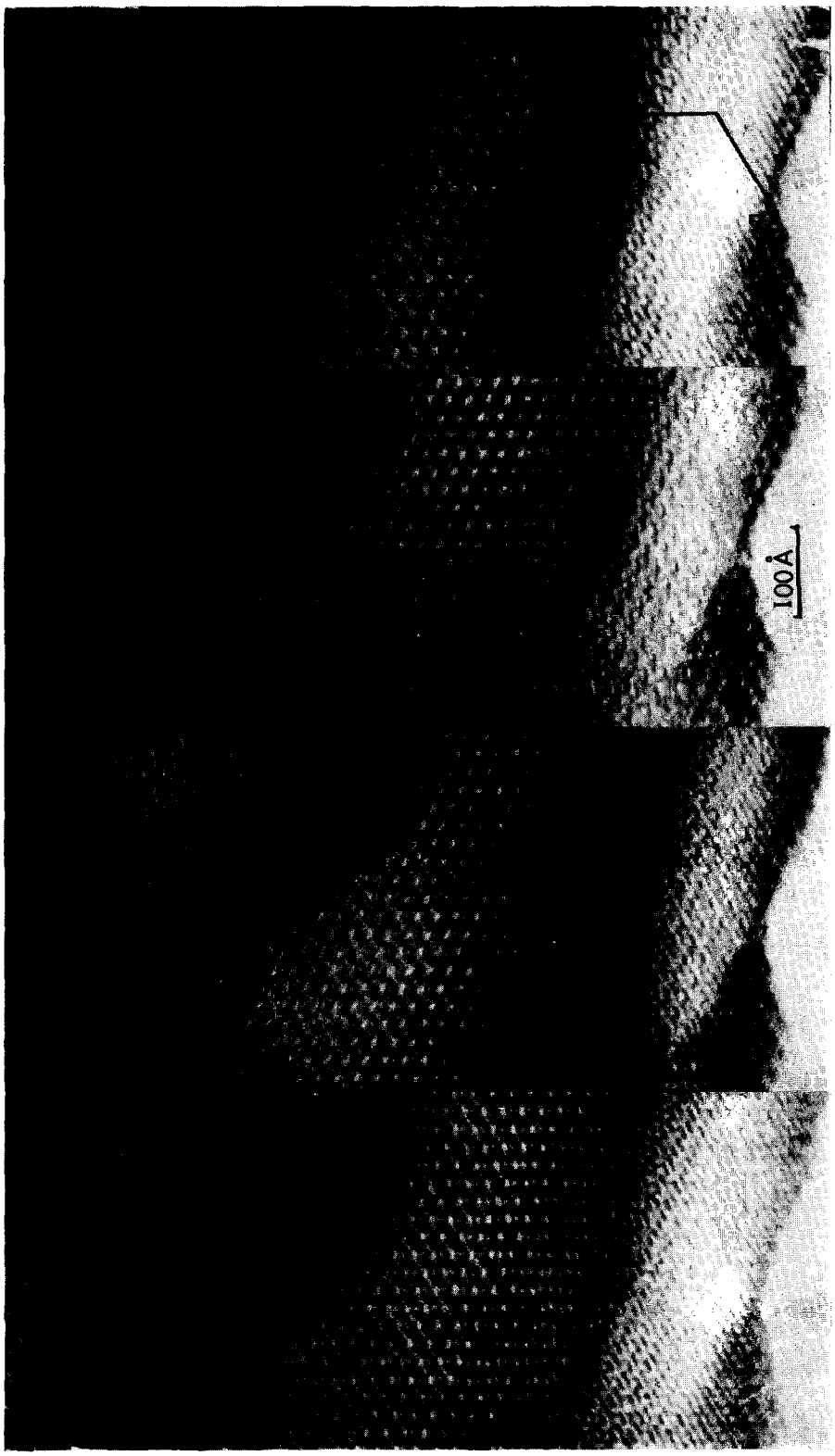

FIG. 14. (*h0l*) lattice images of H-Nb_2O_5, showing the effects of thickness and focus. The crystal is probably wedge shaped. The micrographs were taken with focal increments of about 500 Å.

is a close qualitative agreement between the fringe pattern and the projected structure of the crystal. The crystal approximates to a phase object more closely than would have been anticipated. We have discussed the detailed correlation of lattice image contrast with structure in another place (*19*).

Acknowledgment

Our thanks are due to Dr. K. M. Nimmo for assistance in preparing samples, and to the Science Research Council for support of this work.

References

1. J. G. Allpress and A. D. Wadsley, *J. Solid State Chem.* **1**, 28 (1969).
2. J. G. Allpress, *J. Solid State Chem.* **1**, 66 (1969).
3. J. G. Allpress, *J. Solid State Chem.* **2**, 78 (1970).
4. J. G. Allpress and R. S. Roth, *J. Solid State Chem.* **2**, 366 (1970).
5. H. Schäfer, R. Gruehn and F. Schulte, *Angew Chem. Int. Ed. Engl.* **5**, 40 (1966).
6. A. Reisman and F. Holzberg, in "High Temp. Oxides" (A. M. Alpen, Ed.), Part 2, p. 217. Academic Press New York (1970).
7. R. S. Roth, A. D. Wadsley and S. Andersson, *Acta Crystallogr.* **18**, 643 (1965).
8. B. M. Gatehouse and A. D. Wadsley, *Acta Crystallogr.* **17**, 1545 (1964).
9. W. Mertin, S. Andersson and R. Gruehn, *J. Solid State Chem.* **1**, 419 (1970).
10. S. Andersson, *Z. Anorg. Allg. Chem.* **351**, 106 (1967).
11. A. D. Wadsley, *Acta Crystallogr.* **14**, 664 (1961).
12. W. C. T. Dowell, *Optik (Stuttgart)*, **20**, 535 (1963).
13. T. Komoda, *Optik (Stuttgart)*, **21**, 93 (1964).
14. K. Yada and T. Hibi, *J. Electronmicrosc.* **17**, 97 (1968).
15. H. Hashimoto, Mannami and T. Naiki, *Phil. Trans. Roy. Soc. London, Ser. A* **253**, 459, 1033, (1961).
16. J. M. Cowley and A. F. Moodie, *Proc. Phys. Soc. London*, **76**, 378 (1960).
17. E. A. Chidzey, MSc Thesis, Melbourne, 1970.
18. J. G. Allpress, *Mater. Res. Bull.* **4**, 707 (1969).
19. J. L. Hutchison and J. S. Anderson, *Phys. Status Solidi A* **9**, 207 (1972).